mathematics

MDPI

Article

Global Synchronization of Fractional-Order Multi-Delay Coupled Neural Networks with Multi-Link Complicated Structures via Hybrid Impulsive Control

Hongguang Fan [1,2,3], Yue Rao [1], Kaibo Shi [4] and Hui Wen [2,5,*]

1 College of Computer, Chengdu University, Chengdu 610106, China; fanhongguang@cdu.edu.cn (H.F.)
2 Engineering Research Center of Big Data Application in Private Health Medicine, Fujian Province University, Putian 351100, China
3 School of Mathematical and Computational Science, Hunan University of Science and Technology, Xiangtan 411201, China
4 School of Electronic Information and Electrical Engineering, Chengdu University, Chengdu 610106, China
5 New Engineering Industry College, Putian University, Putian 351100, China
* Correspondence: wen_hui81@163.com

Abstract: This study discusses the global asymptotical synchronization of fractional-order multi-delay coupled neural networks (FMCNNs) via hybrid control schemes. In addition to internal delays and different coupling delays, more importantly, multi-link complicated structures are introduced into our model. Unlike most existing works, the synchronization target is not the special solution of an isolated node, and a more universally accepted synchronization goal involving the average neuron states is introduced. A generalized multi-delay impulsive comparison principle with fractional order is given to solve the difficulties resulting from different delays and multi-link structures. To reduce control costs, a pinned node strategy based on the principle of statistical sorting is provided, and then a new hybrid impulsive pinning control method is established. Based on fractional-order impulsive inequalities, Laplace transforms, and fractional order stability theory, novel synchronization criteria are derived to guarantee the asymptotical synchronization of the considered FMCNN. The derived theoretical results can effectively extend the existing achievements for fractional-order neural networks with a multi-link nature.

Keywords: coupled neural network; synchronization; multi-link structure; impulsive pinning control

MSC: 37N35

check for updates

Citation: Fan, H.; Rao, Y.; Shi, K.; Wen, H. Global Synchronization of Fractional-Order Multi-Delay Coupled Neural Networks with Multi-Link Complicated Structures via Hybrid Impulsive Control. *Mathematics* **2023**, *11*, 3051. https://doi.org/10.3390/math11143051

Academic Editor: Quanxin Zhu

Received: 6 June 2023
Revised: 4 July 2023
Accepted: 6 July 2023
Published: 10 July 2023

1. Introduction

In recent decades, the exploration of complex networks has gradually become a hot topic in various fields of science and engineering [1–6]. Generally speaking, complex networks are composed of a great deal of highly interrelated fundamental units and often exhibit complex and diverse dynamics [7,8]. Among those dynamic behaviors, the synchronization state that exists in many natural and artificial systems has become an important indicator for improving some specific performance of the networks. Various kinds of synchronization modes have aroused considerable concerns from research communities due to their potential applications in different aspects [9–11]. For instance, Sheng et al. [11] investigated the finite-time outer synchronization for discrete-time stochastic complex networks under the case of communication delays and possible information loss and applied the derived synchronization results to image encryption.

It is a noteworthy fact that plenty of complex networks in reality, such as traffic networks, social relation networks, and communication networks, are rarely single-link networks [12]. For example, social relationships can be divided into blood relationships, geographical relationships, and occupational relationships based on different classification standards. If we take each type of relationship as a single-link subnetwork, social relation networks can be better modeled by multi-link complex networks. A multi-link neural network contains multiple neural subnetworks, which can enhance its parallel processing ability. By providing redundant paths for signal transmission, the robustness and fault tolerance of the network can be enhanced. Hence, it is valuable to consider the impact of multi-link complicated structures when studying the synchronization ability of neural networks. Up to now, some impressive achievements concerning the dynamic behaviors of multi-link complex networks have been derived [13–15]. Tang et al. [13] formulated a general model of couple-delayed complex networks involving multi-link natures. By utilizing pinning control, the output synchronization and H_∞ output synchronization issues for multi-link complex networks are investigated in [14]. Zheng et al. [15] studied the synchronization of complex multi-link networks including or not including internal delays using intermittent control schemes.

However, most works mainly focus on multi-link complex networks with integer-order calculus. Fractional calculus, as an extension of derivatives and integrals to arbitrary orders, has an advantage over integer calculus in describing real natural phenomena. It not only enriches degrees of freedom but also has several distinct properties incorporating infinite memory and heredity that the integer calculus operator does not possess [16,17]. Moreover, the fundamental feature of the extension operator is nonlocality, which means its future information depends on the current communication and the past communication simultaneously [18]. Until now, multifarious applications of fractional calculus have involved many aspects, such as viscoelastic systems [19,20], applied mathematics [21], and biomedicine [22]. Especially in terms of memory description and genetic characteristics, fractional calculus also plays a positive role in the study of neural networks [23,24]. Recently, several remarkable synchronization outcomes about multi-link networks with fractional order have been obtained [25–28]. For instance, Xu et al. [25] explored the global asymptotic synchronization problem of multi-link impulsive neural networks with a fractional-order Caputo derivative by feedback control schemes under the assumption of no time delays in signal transmission. Yao et al. [26] focused on the synchronization of fractional-order multi-link complex systems based on Lyapunov direct methods and linear matrix inequalities. Jia et al. [27] explored the synchronization of fractional-order multi-link complex networks including uncertainties in finite time. Sakthivel et al. [28] obtained the synchronization criteria for fractional-order multi-link dynamical networks with disturbances by feedback control strategies.

Various time delays unavoidably exist in complex networks due to the limited switching speed and the inherent communication bandwidth between neurons. To obtain a more realistic synchronization result, Velmurugan et al. [29] considered the projective synchronization issues of fractional-order single-link neural networks with a constant delay by using stability theories and linear feedback control methods. Wang et al. [30] studied the existence, uniqueness, and global asymptotic stability of equilibrium points for delayed fractional-order complex networks. In [31], the global synchronization criteria for fractional-order memristive neural networks including time delays was derived by establishing a new fractional-order delayed inequality without impulses. Ramasamy et al. [32] analyzed the dynamic influence of hypergraph links in fractional-order complex systems and obtained that the high-order interaction was conducive to the early synchronization of networks. Peng et al. [33] discussed the global synchronization problem of fractional-order inertial neural networks including time delays by discontinuous feedback control and adaptive control. Based on the quaternion sign function and some new lemmas, Shang et al. [34] studied the synchronization of fractional-order delayed quaternion neural networks in finite time. Pratap et al. [35] analyzed the synchronization condition of fractional-order multi-link neural networks including internal delays and coupling delays by a feedback controller. Existing works [25–28,35] on fractional-order multi-link neural networks assume that there are no coupling delays or possess the same coupling delays for different topologies under continuous feedback control. Due to the impact of multiple different internal and coupling time delays as well as multi-link complicated structures on the stability of fractional-order systems, it is difficult to achieve synchronization goals for such fractional-order systems using discontinuous impulse control, which is also the key issue and the main challenge of this study. Naturally, how to establish the new impulsive delayed comparison principle and design a reasonable hybrid impulsive control strategy to overcome these unfavorable impacts and reduce control costs has become a key issue that needs to be considered in this article.

In view of the preceding discussion, this paper aims to study the synchronization issue of FMCNNs with multi-link complicated structures. The first mission is to construct an appropriate pinned-node strategy and hybrid impulsive control schemes to obtain the global asymptotical synchronization of the comprehensive neural model under discussion in this paper. In addition, there is a great demand for establishing new impulsive comparison principles to overcome difficulties caused by multi-delays and multi-link complicated structures. The contributions of this article can be summarized below. First, the fractional-order neural networks considered in this study include multi-link complicated structures and internal delays as well as coupling delays, and each coupling structure corresponds to a different coupling time delay, which shows our neural model is more generalized than existing works [25–28,35]. Second, a generalized fractional impulsive comparison principle including multi-delays is established to overcome the influence of multiple time delays and multi-link structures on network synchronization. Third, compared with continuous feedback control in [29,31,33,34], a selection strategy for pinned nodes is given by utilizing the principle of statistical sorting, and a novel hybrid impulsive control scheme is established in this paper, which increases communication security and saves control costs. Lastly, novel synchronization criteria are derived under hybrid impulsive pinning control methods to ensure the more universally accepted synchronization of the concerned FMCNN.

Notation 1. *I_n denotes the n-dimensional identity matrix. R^n denotes the n-dimensional real space. $diag\{\cdots\}$ represents a diagonal matrix. For matrices $P \in R^{n\times m}$ and $F \in R^{r\times q}$, $P \otimes F \in R^{nr\times mq}$ can be calculated by*

$$P \otimes F = \begin{bmatrix} p_{11}F & p_{12}F & \cdots & p_{1m}F \\ p_{21}F & p_{22}F & \cdots & p_{2m}F \\ \vdots & \vdots & \ddots & \vdots \\ p_{n1}F & p_{n2}F & \cdots & p_{nm}F \end{bmatrix}.$$

2. Preliminary Knowledge and Network Model

This part first introduces some important definitions and lemmas, then gives a generalized multi-link network model.

Definition 1. *The fractional integral for a function $\mathfrak{g}(t)$ is defined by*

$$I_t^{\mu}\mathfrak{g}(t) = \frac{1}{\Gamma(\mu)}\int_{t_0}^{t}(t-\bar{\tau})^{\mu-1}\mathfrak{g}(\bar{\tau})d\bar{\tau},$$

where $t \geq t_0$, $\Gamma(\cdot)$ is the Gamma function and $\mu > 0$ represents the order.

Definition 2. *The Caputo fractional derivative for a function $\mathfrak{g}(t)$ is defined by*

$${}^{c}D_t^{\mu}\mathfrak{g}(t) = \frac{1}{\Gamma(n-\mu)}\int_{t_0}^{t}(t-\bar{\tau})^{n-\mu-1}\mathfrak{g}^{(n)}(\bar{\tau})d\bar{\tau},$$

where $t \geq t_0$, $0 \leq n-1 < \mu < n$, and $n \in Z_+$. When $0 < \mu < 1$, one can derive

$${}^{c}D_t^{\mu}\mathfrak{g}(t) = \frac{1}{\Gamma(1-\mu)}\int_{t_0}^{t}(t-\bar{\tau})^{-\mu}\mathfrak{g}'(\bar{\tau})d\bar{\tau}.$$

Lemma 1 ([36]). *Assume that all eigenvalues of $C + M$ meet $|arg(\lambda)| > \frac{\pi}{2}$ and the characteristic equation $det(\Delta(s)) = 0$ has no purely imaginary solutions for $\forall\ \tau_{ij} > 0, i, j = 1, 2, ..., n$, one can derive that the zero solution of the system below*

$$^cD_t^\mu Y(t) = MY(t) + Y(t_\tau),\ \mu \in (0, 1),$$

is globally asymptotically stable, where $M = (m_{ij}) \in R^{n\times n}$, $C = (c_{ij}) \in R^{n\times n}$, $Y(t) = (y_1(t), y_2(t)\ , ..., y_n(t))^T$, $Y(t_\tau) = (\sum_{j=1}^n c_{1j}y_j(t - \tau_{1j}), \sum_{j=1}^n c_{2j}y_j(t - \tau_{2j}), ..., \sum_{j=1}^n c_{nj}y_j(t - \tau_{nj}))^T$, $G = (g_{ij}) = (c_{ij}e^{-s\tau_{ij}} + m_{ij}) \in R^{n\times n}, i, j = 1, 2, ..., n$ and $\Delta(s) = s^\mu I_n - G$.

Lemma 2 ([37]). *Suppose that $x(t) \in C([t_0, +\infty), R)$ is differentiable and $0 < \mu < 1$. If there exists a point $t^\star > t_0$ such that $x(t^\star) = 0$ and $x(t) < 0$ for $t_0 \le t < t^\star$, then $^cD_{t^\star}^\mu x(t^\star) > 0$.*

Lemma 3 ([38]). *Let $w(t) \in R^n$ be a derivable function, then one can derive*

$$^cD_t^\mu w^T(t)w(t) \le 2w^T(t)\,^cD_t^\mu w(t),\ t \ge t_0,\ 0 < \mu < 1.$$

Lemma 4. *Assume that functions $\mathfrak{u}(t) \ge 0$ and $\mathfrak{y}(t) \ge 0$ satisfy*

$$\begin{cases} ^cD_t^\mu \mathfrak{u}(t) \le -a\mathfrak{u}(t) + b_1\mathfrak{u}(t - \tau_1(t)) + b_2\mathfrak{u}(t - \tau_2(t)) + \cdots + b_\alpha\mathfrak{u}(t - \tau_\alpha(t)) \\ \qquad\qquad +c\int_{t-\tau(t)}^t \mathfrak{u}(s)ds,\ t \ne t_\sigma, \\ \mathfrak{u}(t_\sigma) \le \epsilon_\sigma \mathfrak{u}(t_\sigma^-),\ \sigma \in Z_+, \\ \mathfrak{u}(t) = \theta(t),\ t \in [t_0 - \tau, t_0], \end{cases} \tag{1}$$

and

$$\begin{cases} ^cD_t^\mu \mathfrak{y}(t) = -a\mathfrak{y}(t) + b_1\mathfrak{y}(t - \tau_1(t)) + b_2\mathfrak{y}(t - \tau_2(t)) + \cdots + b_\alpha\mathfrak{y}(t - \tau_\alpha(t)) \\ \qquad\qquad +c\int_{t-\tau(t)}^t \mathfrak{y}(s)ds,\ t \ne t_\sigma, \\ \mathfrak{y}(t) = \vartheta(t),\ t \in [t_0 - \tau, t_0], \end{cases} \tag{2}$$

where $0 < \mu < 1, 0 \le \tau(t) \le \tau, 0 \le \tau_i(t) \le \tau(i = 1, 2, \cdots, \alpha), 0 < \epsilon_\sigma \le 1$, $a \in R$, and $b_i \ge 0(i = 1, 2, \cdots, \alpha)$. Then, $\theta(t) \le \vartheta(t)$ for $t_0 - \tau \le t \le t_0$ gives that $\mathfrak{u}(t) \le \mathfrak{y}(t)$ for $t \ge t_0$.

Proof. Utilizing mathematical induction, we first demonstrate that $\mathfrak{u}(t) \le \mathfrak{y}(t)$ for $t \in [t_0, t_1)$. Clearly, $\mathfrak{u}(t) \le \mathfrak{y}(t)$ is equivalent to $\mathfrak{u}(t) < \varsigma\mathfrak{y}(t)$ if $\varsigma > 1$ represents an arbitrary scalar. Assume $\mathfrak{u}(t) \le \mathfrak{y}(t)$ for $t \in [t_0, t_1)$ is not right. Since $\theta(t) \le \vartheta(t)$ for $t \in [t_0 - \tau, t_0]$ and the continuity of $\mathfrak{u}(t)$ and $\mathfrak{y}(t)$ on $[t_0, t_1)$, one can find a point $t^\star \in [t_0, t_1)$ such that

$$\begin{cases} \mathfrak{u}(t) < \varsigma\mathfrak{y}(t), t \in [t_0 - \tau, t^\star), \\ \mathfrak{u}(t^\star) = \varsigma\mathfrak{y}(t^\star), \end{cases} \tag{3}$$

where $\varsigma > 1$ denotes an arbitrary scalar. By Lemma 2, we have

$$^cD_{t^\star}^\mu \mathfrak{u}(t^\star) > \varsigma\,^cD_{t^\star}^\mu \mathfrak{y}(t^\star). \tag{4}$$

However, it derives from Equations (1)–(3) that

$$\begin{aligned}
{}^{c}D^{\mu}_{t^{\star}}\mathfrak{u}(t^{\star}) \leq & -a\mathfrak{u}(t^{\star}) + b_1\mathfrak{u}(t^{\star} - \tau_1(t^{\star})) + b_2\mathfrak{u}(t^{\star} - \tau_2(t^{\star})) + \cdots + b_{\alpha}\mathfrak{u}(t^{\star} - \tau_{\alpha}(t^{\star})) \\
& + c\int_{t^{\star}-\tau(t^{\star})}^{t^{\star}} \mathfrak{u}(s)ds \\
\leq & -a\varsigma\mathfrak{y}(t^{\star}) + b_1\varsigma\mathfrak{y}(t^{\star} - \tau_1(t^{\star})) + b_2\varsigma\mathfrak{y}(t^{\star} - \tau_2(t^{\star})) + \cdots + b_{\alpha}\varsigma\mathfrak{y}(t^{\star} - \tau_{\alpha}(t^{\star})) \\
& + c\varsigma\int_{t^{\star}-\tau(t^{\star})}^{t^{\star}} \mathfrak{y}(s)ds \\
= & \varsigma^{c}D^{\mu}_{t^{\star}}\mathfrak{y}(t^{\star}),
\end{aligned} \tag{5}$$

which contradicts Equation (4), and this contradiction shows

$$\mathfrak{u}(t) < \varsigma\mathfrak{y}(t), t \in [t_0, t_1). \tag{6}$$

Setting $\varsigma \to 1$, one can derive that $\mathfrak{u}(t) \leq \mathfrak{y}(t)$ for $t \in [t_0, t_1)$. Assume there exists $h \in Z_+$ such that $\mathfrak{u}(t) \leq \mathfrak{y}(t)$, $t \in [t_{\sigma-1}, t_{\sigma})$, $\sigma = 2, 3, \cdots, h$, then we have $\mathfrak{u}(t) \leq \mathfrak{y}(t)$ for $t_0 - \tau \leq t < t_h$ and $\mathfrak{u}(t_h) \leq \epsilon_h\mathfrak{u}(t_h^-) \leq \epsilon_h\mathfrak{y}(t_h^-) \leq \mathfrak{y}(t_h^-) = \mathfrak{y}(t_h)$. Since $\mathfrak{y}(t)$ is continuous on $[t_0 - \tau, \infty)$, repeating the similar proof stages for $\mathfrak{u}(t) \leq \mathfrak{y}(t)$ on the interval $[t_0, t_1)$, we can get $\mathfrak{u}(t) \leq \mathfrak{y}(t)$ for $t \in [t_h, t_{h+1})$. Consequently, we complete the proof of Lemma 4. □

Consider the following fractional-order multi-delay neural networks including multi-link complicated structures characterized by

$$\begin{aligned}
{}^{c}D^{\mu}_{t}u_k(t) = & -Bu_k(t) + Af(u_k(t)) + Gh(u_k(t-\tau_0)) + \sum_{j=1}^{N}\epsilon_1 V^{(1)}_{kj}\Gamma_1 u_j(t-\tau_1) \\
& + \sum_{j=1}^{N}\epsilon_2 V^{(2)}_{kj}\Gamma_2 u_j(t-\tau_2) + \cdots + \sum_{j=1}^{N}\epsilon_{\alpha} V^{(\alpha)}_{kj}\Gamma_{\alpha} u_j(t-\tau_{\alpha}),
\end{aligned} \tag{7}$$

where $k = 1, 2, ..., N$, and $u_k(t) = (u_{k1}(t), u_{k2}(t), ..., u_{kn}(t))^T \in R^n$ represents the state of neuron k. $B = \text{diag}\{b_1, b_2, ..., b_n\}$ denotes a diagonal matrix with $b_i > 0$. $A = (a_{kj})_{n\times n}$ and $G = (g_{kj})_{n\times n}$ represent the non-delay and delayed connection strength matrices, respectively. $0 < \tau_0 \leq \tau$ and $0 < \tau_m \leq \tau (m = 1, 2, ..., \alpha)$ represent the internal delay and coupling delays, respectively. $f(u_k(t)) = (f_1(u_{k1}(t)), f_2(u_{k2}(t)), ..., f_n(u_{kn}(t)))^T$ and $h(u_k(t-\tau_0)) = (h_1(u_{k1}(t-\tau_0)), h_2(u_{k2}(t-\tau_0)), ..., h_n(u_{kn}(t-\tau_0)))^T$ represent the non-delay and delayed activation functions at time t and $t - \tau_0$, respectively. $\epsilon_m > 0 (m = 1, 2, ..., \alpha)$ is the coupling strength for the mth coupling structure. $\Gamma_m = \text{diag}\{\gamma_{m1}, \gamma_{m2}, ..., \gamma_{mn}\} > 0 (m = 1, 2, ..., \alpha)$ represents the mth inner-link matrix. $V^{(m)} = (V^{(m)}_{kj})_{N\times N}$ $(m = 1, 2, ..., \alpha)$ denotes the mth coupling configuration matrix, where $V^{(m)}_{kj}$ is decided as follows: if there exists an edge between neuron k and neuron j, then $V^{(m)}_{kj} \neq 0$; otherwise, $V^{(m)}_{kj} = 0 (k \neq j)$. Furthermore, $V^{(m)}$ conforms to the diffusive coupling requirement $V^{(m)}_{kk} = -\sum_{j=1, j\neq k}^{N} V^{(m)}_{kj} (k = 1, 2, ..., N)$.

Define $\bar{u}(t) = \frac{1}{N}\sum\limits_{k=1}^{N} u_k(t)$, then we can obtain

$$
\begin{aligned}
{}^{c}D_t^{\mu}\bar{u}(t) =& \frac{1}{N}\sum_{k=1}^{N} {}^{c}D_t^{\mu}u_k(t) \\
=& \frac{1}{N}\sum_{k=1}^{N}\Big[-Bu_k(t)+Af(u_k(t))+Gh(u_k(t-\tau_0))+\sum_{j=1}^{N}\epsilon_1 V_{kj}^{(1)}\Gamma_1 u_j(t-\tau_1) \\
&+\sum_{j=1}^{N}\epsilon_2 V_{kj}^{(2)}\Gamma_2 u_j(t-\tau_2)+\cdots+\sum_{j=1}^{N}\epsilon_\alpha V_{kj}^{(\alpha)}\Gamma_\alpha u_j(t-\tau_\alpha)\Big] \\
=& -\frac{B}{N}\sum_{k=1}^{N}u_k(t)+\frac{1}{N}\sum_{k=1}^{N}Af(u_k(t))+\frac{1}{N}\sum_{k=1}^{N}Gh(u_k(t-\tau_0)) \\
&+\frac{1}{N}\sum_{j=1}^{N}\epsilon_1\Big(\sum_{k=1}^{N}V_{kj}^{(1)}\Big)\Gamma_1 u_j(t-\tau_1)+\frac{1}{N}\sum_{j=1}^{N}\epsilon_2\Big(\sum_{k=1}^{N}V_{kj}^{(2)}\Big)\Gamma_2 u_j(t-\tau_2) \\
&+\cdots+\frac{1}{N}\sum_{j=1}^{N}\epsilon_\alpha\Big(\sum_{k=1}^{N}V_{kj}^{(\alpha)}\Big)\Gamma_\alpha u_j(t-\tau_\alpha) \\
=& -\frac{B}{N}\sum_{k=1}^{N}u_k(t)+\frac{1}{N}\sum_{k=1}^{N}Af(u_k(t))+\frac{1}{N}\sum_{k=1}^{N}Gh(u_k(t-\tau_0)).
\end{aligned}
\tag{8}
$$

It is clear that $\frac{1}{N}\sum_{m=1}^{\alpha}\sum_{j=1}^{N}\epsilon_m\big(\sum_{k=1}^{N}V_{kj}^{(m)}\big)\Gamma_m u_j(t-\tau_m)=0$ on the basis of the definition of $V^{(m)}$, that is $\sum_{k=1}^{N}V_{kj}^{(m)}=0, m=1,2,...,\alpha, j=1,2,...,N.$

Let error vector $z_k(t)=u_k(t)-\frac{1}{N}\sum_{k=1}^{N}u_k(t)$, then one can obtain

$$
\begin{aligned}
{}^{c}D_t^{\mu}z_k(t) =& -Bz_k(t)+Af(u_k(t))-\frac{1}{N}\sum_{k=1}^{N}Af(u_k(t))+Gh(u_k(t-\tau_0)) \\
&-\frac{1}{N}\sum_{k=1}^{N}Gh(u_k(t-\tau_0))+\sum_{m=1}^{\alpha}\epsilon_m\sum_{j=1}^{N}V_{kj}^{(m)}\Gamma_m z_j(t-\tau_m).
\end{aligned}
\tag{9}
$$

Assumption 1. *For activation functions $f_i(\cdot)$ and $h_i(\cdot)$, there exist constants $\psi_i > 0$, $\phi_i > 0$ such that*

$$
\begin{aligned}
|f_i(\chi_1)-f_i(\chi_2)| \le \psi_i|\chi_1-\chi_2|,\ i=1,2,\ldots,n,\ \chi_1\in R, \chi_2\in R, \\
|h_i(\chi_1)-h_i(\chi_2)| \le \phi_i|\chi_1-\chi_2|,\ i=1,2,\ldots,n,\ \chi_1\in R, \chi_2\in R,
\end{aligned}
$$

where $|(\cdot)|$ represents the absolute value.

Definition 3. *Fractional-order neural network Equation (7) realizes synchronization if*

$$
\lim_{t\to\infty}\|u_k(t)-\frac{1}{N}\sum_{k=1}^{N}u_k(t)\|=0,\ k=1,2,\cdots,N.
$$

Remark 1. *Fractional-order neural networks have unique non-locality and finite memory properties, which integer-order systems do not have. For this reason, fractional-order differential systems can better describe various natural phenomena, as they fully utilize all historical information from initial to current states.*

Remark 2. *Existing fractional-order neural networks mainly focus on synchronization with single time delay or a simple single-link structure, and impulsive synchronization issues of fractional-order* *multi-delay coupling neural networks including multi-link complicated structures are rare. The main reason is that multiple delays and multi-link complicated structures significantly impact the system's stability. This study presents a generalized fractional-order impulsive comparison principle including multiple hybrid delays and utilizes hybrid impulsive control schemes to overcome this difficulty.*

To achieve the synchronization target of fractional-order dynamical system (7), consider the following hybrid impulsive pinning controller

$$U_k(t) = U_{0,k}(t) + U_{1,k}(t),\ k = 1, 2, \ldots, N, \tag{10}$$

where the state feedback control item $U_{0,k}(t)$ is

$$U_{0,k}(t) = -F_k z_k(t),\ k = 1, 2, \ldots, N, \tag{11}$$

and the impulsive control item $U_{1,k}(t)$ is

$$U_{1,k}(t) = \begin{cases} \sum\limits_{\sigma=1}^{+\infty} \beta_\sigma z_k(t)\delta(t - t_\sigma), & k \in \mathfrak{D}(t_\sigma), \\ 0, & k \notin \mathfrak{D}(t_\sigma). \end{cases} \tag{12}$$

Here, F_k is the feedback control gain and β_σ denotes the impulsive strength at t_σ. $\delta(\cdot)$ is the Dirac delta function. The impulsive sequences $\{t_\sigma\}$ meet $t_\sigma \longrightarrow +\infty$ as $\sigma \longrightarrow +\infty$. $\mathfrak{D}(t_\sigma) = \{k_1, k_2, \cdots, k_l\} \subset \{1, 2, \cdots, N\}$ represents the set of pinned neurons at $t = t_\sigma$. To obtain concrete $\mathfrak{D}(t_\sigma)$, one can reorder the errors $z_1(t), z_2(t), \cdots, z_N(t)$ by $\|z_{\theta_1}(t)\| \geq \|z_{\theta_2}(t)\| \geq \cdots \geq \|z_{\theta_l}(t)\| \geq \cdots \geq \|z_{\theta_N}(t)\|$, then $\mathfrak{D}(t_\sigma) = \{\theta_1, \theta_2, \cdots, \theta_l\}$. By Equations (9)–(12), one can further derive that

$$\begin{cases} {}^cD_t^\mu z_k(t) = -Bz_k(t) - F_k z_k(t) + Af(u_k(t)) - \frac{1}{N}\sum\limits_{k=1}^{N} Af(u_k(t)) + Gh(u_k(t - \tau_0)) \\ \qquad - \frac{1}{N}\sum\limits_{k=1}^{N} Gh(u_k(t - \tau_0)) + \sum\limits_{m=1}^{\alpha} \epsilon_m \sum\limits_{j=1}^{N} V_{kj}^{(m)} \Gamma_m z_j(t - \tau_m), t \in [t_{\sigma-1}, t_\sigma), \\ z_k(t_\sigma^+) - z_k(t_\sigma^-) = \beta_\sigma z_k(t_\sigma^-), k \in \mathfrak{D}(t_\sigma), \sharp\mathfrak{D}(t_\sigma) = l, \sigma \in Z_+. \end{cases} \tag{13}$$

3. Main Results

Theorem 1. *Under Assumption 1 and $-2 < \beta_\sigma < 0 (\sigma \in Z_+)$, if there exist constants $\xi_m > 0$, $\eta_1 > 0$, and matrix $F > 0$, such that the inequalities below*

(i) $I_N \otimes (-2B + AA^T + \Psi + GG^T + \eta_1 I_n) + \sum_{m=1}^{\alpha} \xi_m^{-1} \epsilon_m (V^{(m)} V^{(m)T} \otimes \Gamma_m \Gamma_m) - 2F \otimes I_n \leq 0$,
(ii) $\sqrt{2} \sum_{m=0}^{\alpha} \rho_m < \eta_1$,

hold, where $\Psi = diag\{\psi_1^2, \psi_2^2, \ldots, \psi_n^2\}, F = diag\{F_1, F_2, \ldots, F_N\}, \rho_0 = \lambda_{\max}(I_N \otimes \Phi)$, $\rho_m = \xi_m \epsilon_m, m = 1, 2, \ldots, \alpha$, and $\Phi = diag\{\phi_1^2, \phi_2^2, \ldots, \phi_n^2\}$, then neural network Equation (7) is asymptotically synchronized via hybrid impulsive controller Equation (10).

Proof. Consider the following function

$$V(t) = \sum_{k=1}^{N} z_k^T(t) z_k(t) = z^T(t) z(t). \tag{14}$$

When $t \in [t_{\sigma-1}, t_\sigma)$, using Lemma 3, one can obtain that

$$
\begin{aligned}
{}^{c}D_t^{\mu}V(t) \leq & 2\sum_{k=1}^{N} z_k^T(t)\,{}^{c}D_t^{\mu} z_k(t) \\
= & 2\sum_{k=1}^{N} z_k^T(t)\Big[-Bz_k(t) - F_k z_k(t) + Af(u_k(t)) - \frac{1}{N}\sum_{k=1}^{N} Af(u_k(t)) \\
& + Gh(u_k(t-\tau_0)) - \frac{1}{N}\sum_{k=1}^{N} Gh(u_k(t-\tau_0)) + \sum_{m=1}^{\alpha}\sum_{j=1}^{N} \epsilon_m V_{kj}^{(m)} \Gamma_m z_j(t-\tau_m)\Big].
\end{aligned} \tag{15}
$$

From $\sum_{k=1}^{N} z_k^T(t) = 0$, one has $\sum_{k=1}^{N} z_k^T(t)A\left[f(\bar{u}(t)) - \frac{1}{N}\sum_{k=1}^{N} f(u_k(t))\right] = 0$ and $\sum_{k=1}^{N} z_k^T(t)G \left[h(\bar{u}(t-\tau_0)) - \frac{1}{N}\sum_{k=1}^{N} h(u_k(t-\tau_0))\right] = 0$. Utilizing Assumption 1, we can then derive the following inequalities

$$
\begin{aligned}
& 2\sum_{k=1}^{N} z_k^T(t)\left[Af(u_k(t)) - \frac{1}{N}\sum_{k=1}^{N} Af(u_k(t))\right] \\
= & 2\sum_{k=1}^{N} z_k^T(t)A[f(u_k(t)) - f(\bar{u}(t))] + 2\sum_{k=1}^{N} z_k^T(t)A\left[f(\bar{u}(t)) - \frac{1}{N}\sum_{k=1}^{N} f(u_k(t))\right] \\
\leq & \sum_{k=1}^{N} z_k^T(t)AA^T z_k(t) + \sum_{k=1}^{N} z_k^T(t)\Psi z_k(t) \\
= & z^T(t)\left[I_N \otimes (AA^T + \Psi)\right]z(t).
\end{aligned} \tag{16}
$$

$$
\begin{aligned}
& 2\sum_{k=1}^{N} z_k^T(t)\left[Gh(u_k(t-\tau_0)) - \frac{1}{N}\sum_{k=1}^{N} Gh(u_k(t-\tau_0))\right] \\
= & 2\sum_{k=1}^{N} z_k^T(t)G[h(u_k(t-\tau_0)) - h(\bar{u}(t-\tau_0))] \\
& + 2\sum_{k=1}^{N} z_k^T(t)G\left[h(\bar{u}(t-\tau_0)) - \frac{1}{N}\sum_{k=1}^{N} h(u_k(t-\tau_0))\right] \\
\leq & \sum_{k=1}^{N} z_k^T(t)GG^T z_k(t) + \sum_{k=1}^{N} z_k^T(t-\tau_0)\Phi z_k(t-\tau_0) \\
= & z^T(t)(I_N \otimes GG^T)z(t) + z^T(t-\tau_0)(I_N \otimes \Phi)z(t-\tau_0).
\end{aligned} \tag{17}
$$

Moreover, using the properties of the Kronecker product of matrices, one can get

$$
\begin{aligned}
& 2\sum_{k=1}^{N} z_k^T(t) \sum_{m=1}^{\alpha}\sum_{j=1}^{N} \epsilon_m V_{kj}^{(m)} \Gamma_m z_j(t-\tau_m) \\
= & 2\sum_{m=1}^{\alpha} \epsilon_m \left[\sum_{k=1}^{N}\sum_{j=1}^{N} V_{kj}^{(m)} z_k^T(t)\Gamma_m z_j(t-\tau_m)\right] \\
= & 2\sum_{m=1}^{\alpha} \epsilon_m z^T(t)(V^{(m)} \otimes \Gamma_m)z(t-\tau_m) \\
\leq & \sum_{m=1}^{\alpha} \xi_m^{-1}\epsilon_m z^T(t)(V^{(m)}V^{(m)T} \otimes \Gamma_m\Gamma_m)z(t) + \sum_{m=1}^{\alpha} \xi_m \epsilon_m z^T(t-\tau_m)z(t-\tau_m).
\end{aligned} \tag{18}
$$

Substituting Equations (16)–(18) into Equation (15) yields

$$
\begin{aligned}
{}^{c}D_t^{\mu}V(t) \leq & z^T(t)\Big[I_N \otimes (-2B + AA^T + \Psi + GG^T + \eta_1 I_n) + \sum_{m=1}^{\alpha} \xi_m^{-1}\epsilon_m (V^{(m)}V^{(m)T} \otimes \Gamma_m\Gamma_m) \\
& - 2F \otimes I_n\Big] z(t) + z^T(t-\tau_0)(I_N \otimes \Phi)z(t-\tau_0) + \sum_{m=1}^{\alpha} \xi_m\epsilon_m z^T(t-\tau_m)z(t-\tau_m) \\
& - z^T(t)(I_N \otimes \eta_1 I_n)z(t) \\
\leq & -\eta_1 V(t) + \rho_0 V(t-\tau_0) + \sum_{m=1}^{\alpha} \rho_m V(t-\tau_m),
\end{aligned}
\tag{19}
$$

where $\rho_0 = \lambda_{\max}(I_N \otimes \Phi)$ and $\rho_m = \xi_m\epsilon_m (m = 1, 2, \ldots, \alpha)$.

When $t = t_\sigma, \sigma \in Z_+$, we can obtain that

$$
\begin{aligned}
V(t_\sigma^+) &= \sum_{k\in\mathfrak{D}(t_\sigma)} z_k^T(t_\sigma^+)z_k(t_\sigma^+) + \sum_{k\notin\mathfrak{D}(t_\sigma)} z_k^T(t_\sigma^+)z_k(t_\sigma^+) \\
&= \sum_{k\in\mathfrak{D}(t_\sigma)} (1+\beta_\sigma)^2 z_k^T(t_\sigma^-)z_k(t_\sigma^-) + \sum_{k\notin\mathfrak{D}(t_\sigma)} z_k^T(t_\sigma^-)z_k(t_\sigma^-).
\end{aligned}
\tag{20}
$$

Let $\beta_\sigma \in (-2, 0), W_\sigma = \frac{N + l\beta_\sigma(\beta_\sigma+2)}{N} \in (0, 1)$, then one can derive

$$
(N-l)(1-W_\sigma) = \Big[W_\sigma - (1+\beta_\sigma)^2\Big] l \geq 0. \tag{21}
$$

Denote $\Pi_1(t_\sigma^-) = \min\{\|z_k(t_\sigma^-)\| : k \in \mathfrak{D}(t_\sigma)\}, \Pi_2(t_\sigma^-) = \max\{\|z_k(t_\sigma^-)\| : k \notin \mathfrak{D}(t_\sigma)\}$, one can further get

$$
\begin{aligned}
(1-W_\sigma)\sum_{k\notin\mathfrak{D}(t_\sigma)} z_k^T(t_\sigma^-)z_k(t_\sigma^-) &\leq (1-W_\sigma)(N-l)\Pi_2^2(t_\sigma^-) \\
&\leq (1-W_\sigma)(N-l)\Pi_1^2(t_\sigma^-) \\
&= [W_\sigma - (1+\beta_\sigma)^2] l \Pi_1^2(t_\sigma^-) \\
&\leq [W_\sigma - (1+\beta_\sigma)^2] \sum_{k\in\mathfrak{D}(t_\sigma)} z_k^T(t_\sigma^-)z_k(t_\sigma^-).
\end{aligned}
\tag{22}
$$

Combining Equations (20) and (22) yields that

$$
\begin{aligned}
V(t_\sigma^+) =& \sum_{k\in\mathfrak{D}(t_\sigma)} [(1+\beta_\sigma)^2 - W_\sigma] z_k^T(t_\sigma^-)z_k(t_\sigma^-) + \sum_{k\in\mathfrak{D}(t_\sigma)} W_\sigma z_k^T(t_\sigma^-)z_k(t_\sigma^-) \\
& + \sum_{k\notin\mathfrak{D}(t_\sigma)} z_k^T(t_\sigma^-)z_k(t_\sigma^-) \\
\leq & (W_\sigma - 1)\sum_{k\notin\mathfrak{D}(t_\sigma)} z_k^T(t_\sigma^-)z_k(t_\sigma^-) + \sum_{k\in\mathfrak{D}(t_\sigma)} W_\sigma z_k^T(t_\sigma^-)z_k(t_\sigma^-) + \sum_{k\notin\mathfrak{D}(t_\sigma)} z_k^T(t_\sigma^-)z_k(t_\sigma^-) \\
= & W_\sigma \sum_{k=1}^{N} z_k^T(t_\sigma^-)z_k(t_\sigma^-) = W_\sigma V(t_\sigma^-),
\end{aligned}
\tag{23}
$$

where $W_\sigma \in (0, 1)$. Combining Equations (19) and (23) gives

$$
\begin{cases}
{}^{c}D_t^{\mu}V(t) \leq -\eta_1 V(t) + \rho_0 V(t-\tau_0) + \sum\limits_{m=1}^{\alpha} \rho_m V(t-\tau_m),\ t \in [t_{\sigma-1}, t_\sigma), \\
V(t_\sigma^+) \leq W_\sigma V(t_\sigma^-).
\end{cases}
\tag{24}
$$

Consider a multi-delay differential system below

$$^{c}D_t^{\mu}\mathcal{X}(t) = -\eta_1\mathcal{X}(t) + \rho_0\mathcal{X}(t-\tau_0) + \sum_{m=1}^{\alpha}\rho_m\mathcal{X}(t-\tau_m), \tag{25}$$

where $\mathcal{X}(t)$ is continuous on $[t_0-\tau, +\infty)$ and it possesses the same initial condition as $V(t)$. Based on Lemma 4 and $0 < W_\sigma < 1$, we have

$$0 \le V(t) \le \mathcal{X}(t). \tag{26}$$

Utilizing the Laplace transformation for fractional system Equation (25) gives

$$\begin{aligned}
& s^{\mu}\mathcal{X}(s) - s^{\mu-1}\mathcal{X}(t_0) \\
=& -\eta_1\mathcal{X}(s) + \rho_0\int_{t_0}^{+\infty} e^{-st}\mathcal{X}(t-\tau_0)dt + \rho_1\int_{t_0}^{+\infty} e^{-st}\mathcal{X}(t-\tau_1)dt + \cdots \\
& + \rho_\alpha\int_{t_0}^{+\infty} e^{-st}\mathcal{X}(t-\tau_\alpha)dt \\
=& -\eta_1\mathcal{X}(s) + \rho_0\int_{t_0-\tau_0}^{+\infty} e^{-s(t+\tau_0)}\mathcal{X}(t)dt + \rho_1\int_{t_0-\tau_1}^{+\infty} e^{-s(t+\tau_1)}\mathcal{X}(t)dt + \cdots \\
& + \rho_\alpha\int_{t_0-\tau_\alpha}^{+\infty} e^{-s(t+\tau_\alpha)}\mathcal{X}(t)dt \\
=& -\eta_1\mathcal{X}(s) + \rho_0 e^{-s\tau_0}\left[\int_{t_0-\tau_0}^{t_0} e^{-st}\mathcal{X}(t)dt + \int_{t_0}^{+\infty} e^{-st}\mathcal{X}(t)dt\right] + \rho_1 e^{-s\tau_1}\left[\int_{t_0-\tau_1}^{t_0} e^{-st}\mathcal{X}(t)dt\right. \\
& \left. + \int_{t_0}^{+\infty} e^{-st}\mathcal{X}(t)dt\right] + \cdots + \rho_\alpha e^{-s\tau_\alpha}\left[\int_{t_0-\tau_\alpha}^{t_0} e^{-st}\mathcal{X}(t)dt + \int_{t_0}^{+\infty} e^{-st}\mathcal{X}(t)dt\right] \\
=& -\eta_1\mathcal{X}(s) + \rho_0 e^{-s\tau_0}\mathcal{X}(s) + \rho_1 e^{-s\tau_1}\mathcal{X}(s) + \cdots + \rho_\alpha e^{-s\tau_\alpha}\mathcal{X}(s) \\
& + \rho_0 e^{-s\tau_0}\int_{t_0-\tau_0}^{t_0} e^{-st}\mathcal{X}(t)dt + \rho_1 e^{-s\tau_1}\int_{t_0-\tau_1}^{t_0} e^{-st}\mathcal{X}(t)dt + \cdots + \rho_\alpha e^{-s\tau_\alpha}\int_{t_0-\tau_\alpha}^{t_0} e^{-st}\mathcal{X}(t)dt.
\end{aligned} \tag{27}$$

By Lemma 1 and Equation (27), one can get

$$det(\Delta(s))\mathcal{X}(s) = s^{\mu-1}\mathcal{X}(t_0) + \rho_0 e^{-s\tau_0}\int_{t_0-\tau_0}^{t_0} e^{-st}\mathcal{X}(t)dt + \cdots + \rho_\alpha e^{-s\tau_\alpha}\int_{t_0-\tau_\alpha}^{t_0} e^{-st}\mathcal{X}(t)dt, \tag{28}$$

where the characteristic polynomial $det(\Delta(s)) = s^{\mu} + \eta_1 - (\rho_0 e^{-s\tau_0} + \rho_1 e^{-s\tau_1} + \cdots + \rho_\alpha e^{-s\tau_\alpha})$. The next goal is to demonstrate that $det(\Delta(s)) = 0$ has no pure imaginary solutions. Assume $s = \mathfrak{b}i = |\mathfrak{b}|(\cos\frac{\pi}{2} + i\sin(\pm\frac{\pi}{2}))$, where $\mathfrak{b} \in R$. Substituting s into $det(\Delta(s)) = 0$ gives

$$(\mathfrak{b}i)^{\mu} + \eta_1 = \sum_{m=0}^{\alpha}\rho_m e^{-\tau_m\mathfrak{b}i}. \tag{29}$$

Then, one can further derive

$$|(\mathfrak{b}i)^{\mu} + \eta_1|^2 = |\sum_{m=0}^{\alpha}\rho_m e^{-\tau_m\mathfrak{b}i}|^2, \tag{30}$$

which yields that

$$\begin{aligned}
|\mathfrak{b}|^{2\mu} + 2\eta_1\cos\frac{\mu\pi}{2}|\mathfrak{b}|^{\mu} + \eta_1^2 &= (\sum_{m=0}^{\alpha}\rho_m\cos\mathfrak{b}\tau_m)^2 + (\sum_{m=0}^{\alpha}\rho_m\sin\mathfrak{b}\tau_m)^2 \\
&\le 2(\sum_{m=0}^{\alpha}\rho_m)^2.
\end{aligned} \tag{31}$$

Let $\Upsilon(\mathfrak{d}) = \mathfrak{d}^2 + 2\eta_1 \cos\frac{\mu\pi}{2}\mathfrak{d} + \eta_1^2 - (\sum_{m=0}^{\alpha}\rho_m \cos\mathfrak{b}\tau_m)^2 - (\sum_{m=0}^{\alpha}\rho_m \sin\mathfrak{b}\tau_m)^2$. It is not difficult to derive that $\Upsilon(0) = \eta_1^2 - (\sum_{m=0}^{\alpha}\rho_m \cos\mathfrak{b}\tau_m)^2 - (\sum_{m=0}^{\alpha}\rho_m \sin\mathfrak{b}\tau_m)^2 > 0$, since $\sqrt{2}\sum_{m=0}^{\alpha}\rho_m < \eta_1$ and $\rho_m > 0$. Note that $\Upsilon(\mathfrak{d})$ represents a second-order polynomial, and one has $\Upsilon(|\mathfrak{b}|^\mu) > 0$, which indicates the equation in (31) has no solution. Hence, $det(\Delta(s)) = 0$ has no pure imaginary solutions. Moreover, when $\sqrt{2}\sum_{m=0}^{\alpha}\rho_m < \eta_1$, we have $|\arg(-\eta_1 + \sum_{m=0}^{\alpha}\rho_m)| > \frac{\pi}{2}$. Using Lemma 1, the zero solution of Equation (25) is asymptotically stable and $\lim_{t\to+\infty}\mathcal{X}(t) = 0$. Then one can get $\lim_{t\to+\infty}V(t) = 0$ by inequality Equation (26). Hence, the synchronization of multi-link system Equation (7) can be achieved via hybrid impulsive controller Equation (10). □

Remark 3. *Compared with the existing literature concerning fractional-order multi-link systems [25–28,35], our model not only considers internal and coupling time delays but also has different coupling time delays for each coupling structure.*

Based on the theoretical analysis of Theorem 1, when $V^{(2)} = V^{(3)} = \cdots = V^{(m)} = 0$, fractional-order multi-link network Equation (7) is simplified to the following single-link version:

$$^{c}D_t^{\mu}u_k(t) = -Bu_k(t) + Af(u_k(t)) + Gh(u_k(t-\tau_0)) + \sum_{j=1}^{N}\epsilon_1 V_{kj}^{(1)}\Gamma_1 u_j(t-\tau_1), \tag{32}$$

where $k = 1, 2, \cdots, N$. Accordingly, the hybrid impulsive controller for this model is still as shown in Equation (10), then one can derive the following useful corollary.

Corollary 1. *Under Assumption 1 and $-2 < \beta_\sigma < 0(\sigma \in Z_+)$, if there exist constants $\xi_1 > 0, \eta_1 > 0$, and matrix $F > 0$, such that the inequalities below*

(i) $I_N \otimes (-2B + AA^T + \Psi + GG^T + \eta_1 I_n) + \xi_1^{-1}\epsilon_1(V^{(1)}V^{(1)T} \otimes \Gamma_1\Gamma_1) - 2F \otimes I_n \leq 0$,

(ii) $\rho_0 + \rho_1 < \eta_1 \sin\dfrac{\mu\pi}{2}$,

hold, where $\Psi = diag\{\psi_1^2, \psi_2^2, \ldots, \psi_n^2\}, F = diag\{F_1, F_2, \ldots, F_N\}, \rho_0 = \lambda_{\max}(I_N \otimes \Phi)$, $\rho_1 = \xi_1\epsilon_1$, and $\Phi = diag\{\phi_1^2, \phi_2^2, \ldots, \phi_n^2\}$, then single-link neural network Equation (32) is asymptotically synchronized via hybrid impulsive controller Equation (10).

Proof. Similarly to Equation (29), it is not difficult to get the following characteristic equation

$$(\mathfrak{b}i)^\mu + \eta_1 = \rho_0 e^{-\tau_0\mathfrak{b}i} + \rho_1 e^{-\tau_1\mathfrak{b}i}. \tag{33}$$

Substituting $s = \mathfrak{b}i = |\mathfrak{b}|(\cos\frac{\pi}{2} + i\sin(\pm\frac{\pi}{2}))$ into Equation (33), one can derive

$$\begin{cases} |\mathfrak{b}|^\mu \cos\frac{\mu\pi}{2} + \eta_1 = \rho_0\cos(\tau_0\mathfrak{b}) + \rho_1\cos(\tau_1\mathfrak{b}), \\ |\mathfrak{b}|^\mu \sin(\pm\frac{\mu\pi}{2}) = -\rho_0\sin(\tau_0\mathfrak{b}) - \rho_1\sin(\tau_1\mathfrak{b}), \end{cases} \tag{34}$$

which gives

$$|\mathfrak{b}|^{2\mu} + 2\eta_1|\mathfrak{b}|^\mu\cos\frac{\mu\pi}{2} + \eta_1^2 - (\rho_0^2 + \rho_1^2 + 2\rho_0\rho_1\cos\mathfrak{b}(\tau_0 - \tau_1)) = 0. \tag{35}$$

Let $\Upsilon(\mathfrak{d}) = \mathfrak{d}^2 + 2\eta_1\cos\frac{\mu\pi}{2}\mathfrak{d} + \eta_1^2 - (\rho_0^2 + \rho_1^2 + 2\rho_0\rho_1\cos\mathfrak{b}(\tau_0 - \tau_1))$. It is not difficult to derive that $\Upsilon(0) = \eta_1^2 - (\rho_0^2 + \rho_1^2 + 2\rho_0\rho_1\cos\mathfrak{b}(\tau_0 - \tau_1)) > 0$, since $\rho_0 + \rho_1 < \eta_1\sin\frac{\mu\pi}{2}, 0 <$

$\mu < 1$, and $\eta_1 > 0$. By utilizing the properties of $\Upsilon(\mathfrak{d})$ as a second-order polynomial, one can obtain $\Upsilon(|\mathfrak{b}|) > 0$, which shows Equation (35) has no solution and characteristic Equation (33) has no pure imaginary solutions. The remaining proof process is similar to Theorem 1 and we finish the proof of this corollary. □

Remark 4. *Theorem 1 and Corollary 1 are also correct for $\mu = 1$, namely, the synchronization results obtained in this article still hold for integer-order neural networks.*

Remark 5. *According to the results in Theorem 1 and Corollary 1, one can summarize the algorithm steps of the hybrid impulsive control below.*
Step 1. Initialize the system parameters $B, A, G, \mu, \tau_0, \tau_m, \epsilon_m, \Gamma_m, V^{(m)}$.
Step 2. Compute the parameters ϕ_i, ψ_i based on Assumption 1.
Step 3. Choose an appropriate impulse gain β_σ and impulse interval $t_k - t_{k-1}$.
Step 4. Determine the feedback gain F_k and constant parameters η_1, ξ_m based on control conditions.

4. Numerical Examples

This part gives numerical simulations to test the rationality of the achieved theoretical results.

Example 1. *Consider fractional-order multi-delay coupled neural networks including multi-link complicated structures consisting of six neurons, which can be described as*

$$\begin{aligned} {}^{c}D_t^{\mu} u_k(t) =& - Bu_k(t) + Af(u_k(t)) + Gh(u_k(t-\tau_0)) + \sum_{j=1}^{6} \epsilon_1 V_{kj}^{(1)} \Gamma_1 u_j(t-\tau_1) \\ &+ \sum_{j=1}^{6} \epsilon_2 V_{kj}^{(2)} \Gamma_2 u_j(t-\tau_2) + \sum_{j=1}^{6} \epsilon_3 V_{kj}^{(3)} \Gamma_3 u_j(t-\tau_3), \end{aligned} \tag{36}$$

where $\epsilon_1 = 0.5$, $\epsilon_2 = 0.6$, $\epsilon_3 = 0.7$, $\mu = 0.99$, $\tau_0 = 0.05$, $\tau_1 = 0.06$, $\tau_2 = 0.08$, and $\tau_3 = 0.10$. The self-feedback weight matrix and the connection strength matrices are selected as

$$B = \begin{bmatrix} 7.0 & 0 \\ 0 & 7.0 \end{bmatrix}, \ A = \begin{bmatrix} 1.2 & -0.3 \\ -1.0 & 1.2 \end{bmatrix}, \ G = \begin{bmatrix} 0.7 & 0.8 \\ 0.6 & -1.0 \end{bmatrix},$$

respectively. The inner coupling matrices are chosen as

$$\Gamma_1 = \begin{bmatrix} 0.5 & 0 \\ 0 & 0.5 \end{bmatrix}, \ \Gamma_2 = \begin{bmatrix} 1.0 & 0 \\ 0 & 1.0 \end{bmatrix}, \Gamma_3 = \begin{bmatrix} 1.2 & 0 \\ 0 & 1.2 \end{bmatrix}.$$

Moreover, the coupling configuration matrices of fractional-order multi-link system Equation (36) are defined as

$$V^1 = \begin{bmatrix} -0.7 & 0.1 & 0 & 0.3 & 0 & 0.4 \\ 0.1 & -0.9 & 0.6 & 0 & 0.2 & 0 \\ 0 & 0.6 & -1.4 & 0.7 & 0 & 0.1 \\ 0.3 & 0 & 0.7 & -1.1 & 0.1 & 0 \\ 0 & 0.2 & 0 & 0.1 & -0.6 & 0.3 \\ 0.4 & 0 & 0.1 & 0 & 0.3 & -0.8 \end{bmatrix},$$

$$V^2 = \begin{bmatrix} -0.8 & 0.25 & 0 & 0 & 0.2 & 0.35 \\ 0.25 & -0.7 & 0.15 & 0.3 & 0 & 0 \\ 0 & 0.15 & -0.85 & 0.2 & 0.1 & 0.4 \\ 0 & 0.3 & 0.2 & -1.0 & 0.5 & 0 \\ 0.2 & 0 & 0.1 & 0.5 & -1.15 & 0.35 \\ 0.35 & 0 & 0.4 & 0 & 0.35 & -1.1 \end{bmatrix},$$

$$V^3 = \begin{bmatrix} -1.1 & 0.25 & 0.15 & 0.4 & 0.3 & 0 \\ 0.25 & -1.25 & 0.25 & 0.35 & 0 & 0.4 \\ 0.15 & 0.25 & -1.7 & 0.55 & 0.65 & 0.1 \\ 0.4 & 0.35 & 0.55 & -2.5 & 0.85 & 0.35 \\ 0.3 & 0 & 0.65 & 0.85 & -2.25 & 0.45 \\ 0 & 0.4 & 0.1 & 0.35 & 0.45 & -1.3 \end{bmatrix}.$$

The non-delay and delayed activation functions are $f_i(x) = h_i(x) = \tanh(x)$. It is clear that Assumption 1 holds when $\phi_i = \psi_i = 1 (i = 1, 2)$. Let $\eta_1 = 4.25$, $F_k = 4.78$, $t_\sigma - t_{\sigma-1} = 0.05$, and $\xi_m = 1 (m = 1, 2, 3)$. A simple calculation gives that $\sqrt{2}\sum_{m=0}^{\alpha} \rho_m - \eta_1 = -0.2902 < 0$, and the maximum eigenvalue of matrix $\Omega = I_N \otimes (-2B + AA^T + \Psi + GG^T + \eta_1 I_n) + \sum_{m=1}^{\alpha} \xi_m^{-1} \epsilon_m (V^{(m)} V^{(m)T} \otimes \Gamma_m \Gamma_m) - 2F \otimes I_n$ is $-0.4353 < 0$. Consequently, the above parameters fulfill all the requirements in Theorem 1. The initial values of multi-link network Equation (36) are randomly chosen within the real interval $[-5\ \ 5]$. Utilizing the hybrid impulsive control methods, the time evolution processes of $u_k(t)$ and $z_k(t)$ can be seen in Figure 1a,b under the above control parameters. The horizontal ordinate in the figure represents the system's evolution time. Figure 1a displays that the two dimension states of vectors $u_k(t)$ of all neurons tend to converge to completely consistent states over time. Figure 1b displays that the error norm of neurons gradually approaches zero as the control duration increases. Based on the definition of global synchronization, Figure 1 shows that the controlled multi-link network can achieve global asymptotical synchronization, which means the theoretical analysis of Theorem 1 is correct.

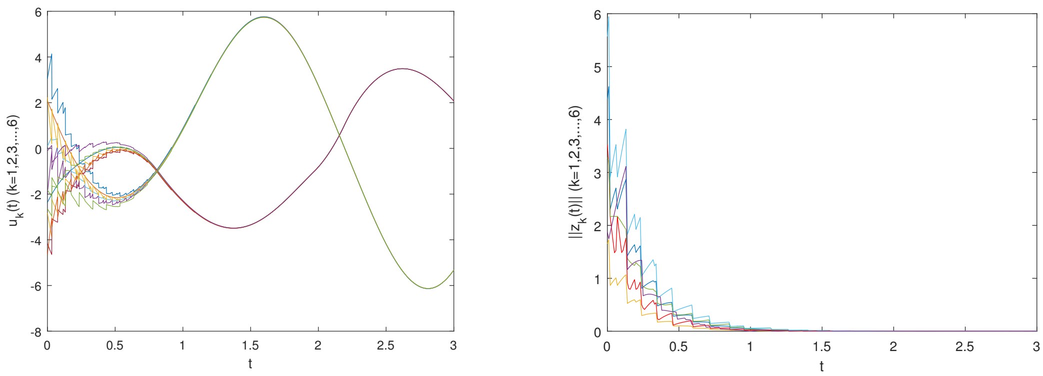

(**a**) (**b**)

Figure 1. The time evolution processes of $u_k(t)$ and $\|z_k(t)\|$ under hybrid impulsive control in Example 1. (**a**) $u_k(t)$; (**b**) $\|z_k(t)\|$.

Remark 6. *In contrast to the continuous feedback control in [29,31,33,34], hybrid impulsive control, as a class of discontinuous control methods, can carry on impulse stimulation at impulse instants and feedback stimulation within the impulse interval, which possesses the merits of simple implementation and increased safety during signal transmission. Comparing pure impulsive control [7,9,16] with the method presented in this article, if pure impulsive control is used instead of hybrid impulsive control, one can find that condition (i) in Theorem 1 is always untenable, since the feedback part $F \otimes I_n$ is the key factor in the validity of condition (i).*

Remark 7. *Considering the nonlocality of fractional differential equations, a typical predictor-corrector scheme called Adams–Bashforth–Moulton [39] has been used for solving multi-delay fractional-order differential equations in a numerical simulation in Matlab R2020b (see Appendix A). We should point out that one can apply the product trapezoidal quadrature rule for the corrector term and use the product rectangle rule to evaluate the predictor term. Hence, with the help of these two rules and the given algorithm steps, the entire numerical method is easy to implement.*

Example 2. *Consider fractional-order coupled neural networks including single-link topological structures described as*

$$^{c}D_t^{\mu}u_k(t) = -Bu_k(t) + Af(u_k(t)) + Gh(u_k(t-\tau_0)) + \sum_{j=1}^{6}\epsilon_1 V_{kj}^{(1)}\Gamma_1 u_j(t-\tau_1), \tag{37}$$

where $\epsilon_1 = 0.8$, $\mu = 0.95$, $\tau_0 = 0.03$, *and* $\tau_1 = 0.04$. *The self-feedback weight matrix and the connection strength matrices are selected as*

$$B = \begin{bmatrix} 4.0 & 0 \\ 0 & 15 \end{bmatrix},\ A = \begin{bmatrix} 1.6 & -1.8 \\ 1.8 & 1.4 \end{bmatrix},\ G = \begin{bmatrix} -1.0 & 1.0 \\ 3.0 & -3.0 \end{bmatrix},$$

respectively. The inner coupling matrix and the coupling configuration matrix are chosen as

$$\Gamma_1 = \begin{bmatrix} 1.0 & 0 \\ 0 & 1.0 \end{bmatrix},\ V^1 = \begin{bmatrix} -1.4 & 0.2 & 0.4 & 0.3 & 0.1 & 0.4 \\ 0.2 & -1.8 & 0.6 & 0.2 & 0.5 & 0.3 \\ 0.4 & 0.6 & -1.6 & 0.3 & 0.1 & 0.2 \\ 0.3 & 0.2 & 0.3 & -1.9 & 0.9 & 0.2 \\ 0.1 & 0.5 & 0.1 & 0.9 & -2.0 & 0.4 \\ 0.4 & 0.3 & 0.2 & 0.2 & 0.4 & -1.5 \end{bmatrix},$$

respectively.

The non-delay and delayed activation functions are $f_i(x) = h_i(x) = 0.5\tanh(x)$. It is clear that Assumption 1 holds when $\phi_i = \psi_i = 0.5$. Let $\eta_1 = 1.61$, $F_k = 6.26$, $t_\sigma - t_{\sigma-1} = 0.1$, and $\xi_1 = 1$. A simple calculation gives that $\rho_0 + \rho_1 - \eta_1 \sin\frac{\mu\pi}{2} = -0.3050 < 0$, and the maximum eigenvalue of matrix $\Omega = I_N \otimes (-2B + AA^T + \Psi + GG^T + \eta_1 I_n) + \xi_1^{-1}\epsilon_1(V^{(1)}V^{(1)T} \otimes \Gamma_1\Gamma_1) - 2F \otimes I_n$ is $-0.2812 < 0$. Hence, the above parameters guarantee all the requirements in Corollary 1 are fulfilled. The initial states of fractional-order single-link network Equation (37) are randomly selected within the interval $[-5\ \ 5]$. Under the hybrid impulsive control schemes, the simulation results of $u_k(t)$ and $z_k(t)$ in Equation (37) are given in Figure 2a,b. The abscissa in the figure also stands for the system's evolution time. Figure 2a indicates that the two-dimensional state vectors $u_k(t)$ of all network nodes tend to converge to a completely consistent state over control time. Figure 2b indicates that the error norm of all network nodes gradually approaches zero as the control duration increases. Figure 2 shows that single-link neural network Equation (37) can achieve asymptotical synchronization under the proposed hybrid control schemes, which validates Corollary 1.

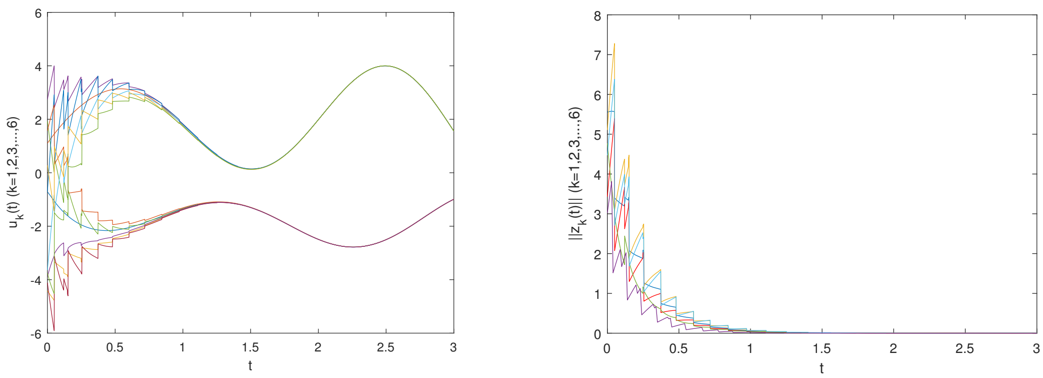

(**a**) (**b**)

Figure 2. The time evolution processes of $u_k(t)$ and $\|z_k(t)\|$ under hybrid impulsive control in Example 2. (**a**) $u_k(t)$; (**b**) $\|z_k(t)\|$.

5. Conclusions

This article analyzed and validated the global asymptotical synchronization of fractional-order multi-delay coupled neural networks (FMCNNs). Due to the impact of various time delays and multi-link structures on the stability of fractional-order complex systems, this paper addressed these difficulties by establishing a generalized fractional-order comparison lemma and a hybrid impulsive pinning control strategy, and some new sufficient conditions were acquired to ensure the global synchronization of the concerned multi-delay coupled neural networks. We will combine event-triggering strategies and impulsive pinning control technologies to achieve the selection of impulse instants and network nodes in the future. In addition, as an important tool, the theory of fixed points could be applied to impulsive synchronization analyses. This is also a worthwhile direction for our future research.

Author Contributions: Conceptualization, H.F., K.S. and H.W.; methodology, K.S. and H.W.; software, H.F., Y.R. and H.W.; writing—original draft, H.F., Y.R. and K.S.; writing—review and editing, H.F., Y.R., K.S. and H.W. All authors have read and agreed to the published version of the manuscript.

Funding: This work was supported by the Open Foundation of Engineering Research Center of Big Data Application in Private Health Medicine, Fujian Province University under Grant (MKF202201), the Sichuan Science and Technology Program under Grant (21YYJC0469), the Program of Science and Technology of Sichuan Province of China under Grant (2021ZYD0012), and the Natural Science Foundation of Fujian Province under Grant (2019J01815, 2022J011171, 2022J011170).

Institutional Review Board Statement: Not applicable.

Informed Consent Statement: Not applicable.

Data Availability Statement: Not applicable.

Conflicts of Interest: The authors declare no conflict of interest.

Appendix A

To facilitate the readers' understanding of the solution of the fractional-order differential equation in this paper, we have provided the following relevant code, which is named fo_solution.m.

```
function [t,y] = fo_solution(step,tfinal,ini_value,mu,delay)
len = length(ini_value);
N = tfinal/step;
t = linspace(0,N,N + 1)*step;
k = delay/step;
y0 = ini_value;
y = zeros(len,N);
for n = 0:N − 1
disp(['execution number:', num2str(n), 't = ', num2str(n*step)]);
b=@(j) step^mu/mu * ((n+1-j)^mu - (n-j)^mu);
s = zeros(len,1);
for j = 0 : n
if j - k <= 0
x_jk = y0;
else
x_jk = y(:, j - k);
end
if j == 0
x_j = y0;
else
x_j = y(:, j);
end
s = s + b(j) * equ(j * step, x_j, x_jk);
```

end
$yp = y0 + s/gamma(mu);$
$a = @(j)(n-j+2)^{(mu+1)} + (n-j)^{(mu+1)} - 2*(n-j+1)^{(mu+1)};$
$SUM0 = (n^{(mu+1)} - (n-mu)*(n+1)^{mu})*equ(0, y0, y0);$
$SUM1 = zeros(len, 1);$
$for\ j = 1 : n$
$if\ j - k <= 0$
$x_{jk} = y0;$
$else$
$x_{jk} = y(:, j-k);$
end
$x_j = y(:, j);$
$SUM1 = SUM1 + a(j)*equ(j*step, x_j, x_{jk});$
end
$SUM = SUM0 + SUM1;$
$if\ n + 1 - k <= 0$
$x_{nk} = y0;$
$else$
$x_{nk} = y(:, n+1-k);$
end
$y(:, n+1) = y0 + step^{mu}/gamma(mu+2)*equ(n*step, yp, x_{nk}) + SUM*step^{mu}/$
$gamma(\mathrm{mu}+2);$
end
$y = [y0, y];$
end

References

1. Wang, F.; Yang, Y.Q.; Hu, M.F.; Xu, X.Y. Projective cluster synchronization of fractional-order coupled-delay complex network via adaptive pinning control. *Physica* **2015**, *434*, 134–143. [CrossRef]
2. Ding, K.; Zhu, Q.X. A note on sampled-data synchronization of memristor networks subject to actuator failures and two different activations. *IEEE Trans. Circuits Syst. II Express Briefs* **2021**, *68*, 2097–2101. [CrossRef]
3. Kong, F.C.; Zhu, Q.X.; Huang, T.W. Fixed-time stability for discontinuous uncertain inertial neural networks with time-varying delays. *IEEE Trans. Syst. Man Cybern. Syst.* **2022**, *52*, 4507–4517. [CrossRef]
4. Zhu, Q.X.; Huang, T.W. H_∞ control of stochastic networked control systems with time-varying delays: The event-triggered sampling case. *Int. J. Robust Nonlinear Control* **2021**, *31*, 9767–9781. [CrossRef]
5. Zhao, Y.; Zhu, Q.X. Stabilization of stochastic highly nonlinear delay systems with neutral term. *IEEE Trans. Autom. Control* **2023**, *68*, 2544–2551. [CrossRef]
6. Zhong, Q.S.; Han, S.; Shi, K.B.; Zhong, S.M.; Kwon, O.M. Co-design of adaptive memory event-triggered mechanism and aperiodic intermittent controller for nonlinear networked control systems. *IEEE Trans. Circuits Syst.—II Express Briefs* **2022**, *69*, 4979–4983. [CrossRef]
7. Fan, H.G.; Shi, K.B.; Zhao, Y. Pinning impulsive cluster synchronization of uncertain complex dynamical networks with multiple time-varying delays and impulsive effects. *Physica* **2022**, *587*, 126534. [CrossRef]
8. Zhu, Q.X. Stabilization of stochastic nonlinear delay systems with exogenous disturbances and the event-triggered feedback control. *IEEE Trans. Autom. Control* **2019**, *64*, 3764–3771. [CrossRef]
9. Fan, H.G.; Xiao, Y.; Shi, K.B.; Wen, H.; Zhao, Y. μ-synchronization of coupled neural networks with hybrid delayed and non-delayed impulsive effects. *Chaos Solitons Fractals* **2023**, *173*, 113620. [CrossRef]
10. Jiang, C.H.; Tang, Z.; Park, J.H.; Xiong, N.N. Matrix measure-based projective synchronization on coupled neural networks with clustering trees. *IEEE Trans. Cybern.* **2023**, *53*, 1222–1234. [CrossRef]
11. Sheng, S.Y.; Zhang, X.M.; Lu, G.P. Finite-time outer-synchronization for complex networks with Markov jump topology via hybrid control and its application to image encryption. *J. Frankl. Inst.* **2018**, *355*, 6493–6519. [CrossRef]
12. Fan, H.G.; Tang, J.H.; Shi, K.B.; Zhao, Y.; Wen, H. Delayed impulsive control for μ-synchronization of nonlinear multi-weighted complex networks with uncertain parameter perturbation and unbounded delays. *Mathematics* **2023**, *11*, 250. [CrossRef]
13. Tang, Y.; Zhou, L.; Tang, J.H.; Rao, Y.; Fan, H.G.; Zhu, J.H. Hybrid impulsive pinning control for mean square synchronization of uncertain multi-link complex networks with stochastic characteristics and hybrid delays. *Mathematics* **2023**, *11*, 1697. [CrossRef]
14. Wang, J.L.; Qin, Z.; Wu, H.N.; Huang, T.W.; Wei, P.C. Analysis and pinning control for output synchronization and H_∞ output synchronization of multi-weighted complex networks. *IEEE Trans. Cybern.* **2019**, *49*, 1314–1326. [CrossRef]

15. Zheng, M.W.; Li, L.X.; Peng, H.P.; Xiao, J.H.; Yang, Y.X.; Zhao, H.; Ren, J.F. Finite-time synchronization of complex dynamical networks with multi-links via intermittent controls. *Eur. Phys. J.* **2016**, *89*, 43. [CrossRef]
16. Wang, F.; Zheng, Z.W.; Yang, Y.Q. Quasi-synchronization of heterogenous fractional-order dynamical networks with time-varying delay via distributed impulsive control. *Chaos Solitons Fractals* **2021**, *142*, 110465. [CrossRef]
17. Wang, F.; Zheng, Z.W. Quasi-projective synchronization of fractional order chaotic systems under input saturation. *Physica* **2019**, *534*, 122132. [CrossRef]
18. Yu, N.X.; Zhu, W. Event-triggered impulsive chaotic synchronization of fractional-order differential systems. *Appl. Math. Comput.* **2021**, *388*, 125554. [CrossRef]
19. Peng, W.; Chen, L.; He, T.H. A modified fractional order thermo-viscoelastic theory with fractional order strain and its application in a thermo-viscoelastic problem containing a spherical cavity. *Mech.—Time-Depend. Mater.* **2022**, *26*, 891–907. [CrossRef]
20. Tripathi, D.; Pandey, S.K.; Das, S. Peristaltic flow of viscoelastic fluid with fractional Maxwell model through a channel. *Appl. Math. Comput.* **2010**, *215*, 3645–3654. [CrossRef]
21. Jiang, M.; Zhong, S.M. Successively iterative method for fractional differential equations with integral boundary conditions. *Appl. Math. Lett.* **2014**, *38*, 94–99. [CrossRef]
22. Abbes, A.; Ouannas, A.; Shawagfeh, N.; Grassi, G. The effect of the Caputo fractional difference operator on a new discrete COVID-19 model. *Results Phys.* **2022**, *39*, 105797. [CrossRef] [PubMed]
23. Pratap, A.; Raja, R.; Cao, J.D.; Rihan, F.A.; Seadawy, A.R. Quasi-pinning synchronization and stabilization of fractional order BAM neural networks with delays and discontinuous neuron activations. *Chaos Solitons Fractals* **2020**, *131*, 109491. [CrossRef]
24. Pratap, A.; Raja, R.; Agarwal, R.P.; Cao, J.D. Stability analysis and robust synchronization of fractional-order competitive neural networks with different time scales and impulsive perturbations. *Int. J. Adapt. Control. Signal Process.* **2019**, *33*, 1635–1660. [CrossRef]
25. Xu, Y.; Li, Y.Z.; Li, W.X.; Feng, J.Q. Synchronization of multi-links impulsive fractional-order complex networks via feedback control based on discrete-time state observations. *Neurocomputing* **2020**, *406*, 224–233. [CrossRef]
26. Bao, H.B.; Cao, J.D. Projective synchronization of fractional-order memristor-based neural networks. *Neural Netw.* **2015**, *63*, 1–9. [CrossRef]
27. Jia, Y.; Wu, H.Q.; Cao, J.D. Non-fragile robust finite-time synchronization for fractional-order discontinuous complex networks with multi-weights and uncertain couplings under asynchronous switching. *Appl. Math. Comput.* **2020**, *370*, 124929. [CrossRef]
28. Sakthivel, R.; Sakthivel, R.; Kwon, O.M.; Selvaraj, P.; Anthoni, S.M. Observer-based robust synchronization of fractional-order multi-weighted complex dynamical networks. *Nonlinear Dyn.* **2019**, *98*, 1231–1246. [CrossRef]
29. Velmurugan, G.; Rakkiyappan, R. Hybrid projective synchronization of fractional-order memristor-based neural networks with time delays. *Nonlinear Dyn.* **2016**, *83*, 419–432. [CrossRef]
30. Wang, F.; Yang, Y.; Hu, M. Asymptotic stability of delayed fractional-order neural networks with impulsive effects. *Neurocomputing* **2015**, *154*, 239–244. [CrossRef]
31. Chen, L.P.; Cao, J.D.; Wu, R.C.; Machado, J.A.T.; Lopes, A.M.; Yang, H.J. Stability and synchronization of fractional-order memristive neural networks with multiple delays. *Neural Netw.* **2017**, *94*, 76–85. [CrossRef] [PubMed]
32. Ramasamy, M.; Kumarasamy, S.; Srinivasan, A.; Subburam, P.; Rajagopal, K. Dynamical effects of hypergraph links in a network of fractional-order complex systems. *Chaos* **2022**, *32*, 123128. [CrossRef]
33. Peng, Q.; Jian, J.G. Synchronization analysis of fractional-order inertial-type neural networks with time delays. *Math. Comput. Simul.* **2023**, *205*, 62–77. [CrossRef]
34. Shang, W.Y.; Zhang, W.W.; Chen, D.Y.; Cao, J.D. New criteria of finite time synchronization of fractional-order quaternion-valued neural networks with time delay. *Appl. Math. Comput.* **2023**, *436*, 127484. [CrossRef]
35. Pratap, A.; Raja, R.; Agarwal, R.P.; Cao, J.D.; Bagdasar, O. Multi-weighted complex structure on fractional order coupled neural networks with linear coupling delay: A robust synchronization problem. *Neural Process. Lett.* **2020**, *51*, 2453–2479. [CrossRef]
36. Wang, H.; Yu, Y.G.; Wen, G.G.; Zhang, S.; Yu, J.Z. Global stability analysis of fractional-order Hopfield neural networks with time delay. *Neurocomputing* **2015**, *154*, 15–23. [CrossRef]
37. Liu, P.; Zeng, Z.; Wang, J. Multiple Mittag–Leffler stability of fractional-order recurrent neural networks. *IEEE Trans. Syst. Man Cybern. Syst.* **2017**, *47*, 2279–2288. [CrossRef]
38. Aguila-Camacho, N.; Duarte-Mermoud, M.; Gallegos, J. Lyapunov functions for fractional order systems. *Commun. Nonlinear Sci. Numer. Simul.* **2014**, *19*, 2951–2957. [CrossRef]
39. Bhalekar, S.; Gejji, V. A predictor-corrector scheme for solving nonlinear delay differential equations of fractional order. *J. Fract. Calc. Appl.* **2011**, *5*, 1–9.